SCIENCE CHINA
Information Sciences

• **Supplementary File** •

Digital computation of linear canonical transform for local spectra with flexible resolution ability

Yannan SUN[1,2] & Bingzhao LI[1,2*]

[1]*School of Mathematics and Statistics, Beijing Institute of Technology, Beijing* 100081,*China;*
[2]*Beijing Key Laboratory on MCAACI, Beijing Institute of Technology, Beijing* 100081, *China*

Appendix A Preliminaries

The linear canonical transform(LCT) of the ideal uniform sampled signal $x(t)$ with the sampling interval T is given in [1–4]

$$L_A[x(n)](u) = \sum_{n=-\infty}^{\infty} x(nT)K_A(u,n) = \frac{1}{T}\sum_{n=-\infty}^{\infty} e^{-j\pi\alpha(\frac{n}{T\beta})^2} e^{j2\pi\alpha\frac{un}{T\beta}} L_A[x(t)](u-\frac{n}{T\beta}), \tag{A1}$$

where $K_A(u,n) = \sqrt{\beta}e^{\frac{-j\pi}{4}} e^{j\pi(\alpha u^2 - 2\beta unT + \gamma(nT)^2)}$. Eq.(A1) is defined as the discrete time LCT (DTLCT) [1], which replicates $L_A[x(t)](u)$ with a period of $1/(T|\beta|)$ along with linear phase modulation.

We assume that the signal $x(t)$ is limited in the time domain $[-W/2, W/2]$. Thus, intercepting N terms of (A1), it can be rewritten as

$$L_A[x(n)](u) \approx \sqrt{\beta}e^{-j\pi/4}e^{j\pi\alpha u^2}\sum_{n=-N/2}^{N/2-1} x(n)e^{j\pi\gamma(nT)^2}e^{-j2\pi\beta unT}, \tag{A2}$$

where N is the number of uniform sampling points in the time domain. Without loss of generality, we denote $x(n) = x(nT)$. Since the LCT of the sampled signal is periodic along with linear phase modulation. Therefore, we choose N samples in the range $[-1/(2T|\beta|), 1/(2T|\beta|) - 1/(NT|\beta|)]$ that is unaffected by the chirp periodic factors. We sample $L_A[x(n)](u)$ with sampling interval $T_u = 1/NT|\beta|$. Thus, the DLCT of $x(n)$ can be defined as [1, 3, 5, 6],

$$L_A[x(n)](mT_u) = \sqrt{\beta}e^{-j\pi/4}e^{j\pi\alpha(m/NT|\beta|)^2}\sum_{n=-N/2}^{N/2-1} x(n)e^{j\pi\gamma(nT)^2}e^{-j2\pi\beta mn/(N|\beta|)}, \tag{A3}$$

where $T_u = 1/NT|\beta|$ is standard frequency resolution of LCT, $m = -N/2, -N/2+1, ..., N/2-1$.

Appendix B Proof of Theorem.1

Proof. For $\forall[u_1, u_2] \subseteqq [-1/(2T|\beta|), 1/(2T|\beta|) - 1/(NT|\beta|)]$, we sample uniformly the transform function $L_A[x(n)](u)$ in (A2) with sampling interval $\Delta I = (u_2 - u_1)/M$, and $\Delta I < 1/NT|\beta|$. Let $u_i = (u_1 + u_2)/2$ and substitute $u = u_i + m\Delta I$, $-M/2 \leqslant m \leqslant M/2 - 1$ into (A2), we obtain

$$\begin{aligned}
&L_A[x(n)](u_i + m\Delta I)\\
&= \sqrt{\beta}e^{-i\pi/4}e^{j\pi\alpha(u_i+m\Delta I)^2}\sum_{n=-N/2}^{N/2-1} x(n) \times e^{j\pi\gamma(nT)^2}e^{-j2\pi\beta u_i(nT)}e^{-j2\pi\beta mn\Delta IT}\\
&= \sqrt{\beta}e^{-i\pi/4}e^{j\pi\alpha(u_i+m\Delta I)^2}e^{-j\pi\beta\Delta ITm^2}\sum_{n=-N/2}^{N/2-1} x(n) \times e^{j\pi\gamma(nT)^2}e^{-j2\pi\beta u_i(nT)}e^{-j\pi\beta\Delta ITn^2}e^{j\pi\beta\Delta IT(m-n)^2}.
\end{aligned} \tag{B1}$$

* Corresponding author (email: li_bingzhao@bit.edu.cn)

Based on the definitions of the zoom factor and shift factor, we have $\lambda = u_i(T|\beta|)$, $P = 1/(NT|\beta|\Delta I)$, then substituting $u_i = \lambda/(T|\beta|)$ and $\Delta I = 1/(PNT|\beta|)$ into (B1), we derive that

$$\begin{aligned} &L_A[x(n)](\frac{\lambda}{T|\beta|} + \frac{m}{PNT|\beta|}) \\ &= \sqrt{\beta}e^{-i\pi/4}e^{j\pi\alpha(\frac{\lambda}{T|\beta|}+\frac{m}{PNT|\beta|})^2}e^{-j\pi\frac{Tm^2\beta}{PNT|\beta|}}\sum_{n=-N/2}^{N/2-1} f(n)\times e^{j\pi\gamma(nT)^2}e^{-j2\pi\beta\frac{\lambda}{T|\beta|}(nT)}e^{-j\pi\beta T\frac{n^2}{PNT|\beta|}}e^{j\pi\beta T\frac{(m-n)^2}{NTP|\beta|}}. \end{aligned} \tag{B2}$$

Let $s = \beta/|\beta| = sign(\beta)$, we obtain

$$\begin{aligned} &L_A[x(n)](\frac{\lambda}{T|\beta|} + \frac{m}{PNT|\beta|}) \\ &= \sqrt{\beta}e^{-i\pi/4}e^{j\pi\alpha(\frac{\lambda}{T|\beta|}+\frac{m}{PNT|\beta|})^2}e^{-j\pi s\frac{m^2}{PN}}\times\sum_{n=-N/2}^{N/2-1} x(n)e^{j\pi\gamma(nT)^2}e^{-j2\pi\lambda ns}e^{-j\pi s\frac{n^2}{PN}}e^{j\pi s\frac{(m-n)^2}{NP}}, \end{aligned} \tag{B3}$$

Eq.(B3) can be rewritten as the following matrix form

$$\boldsymbol{L}_A = \sqrt{\beta}e^{-j\pi/4}\boldsymbol{x}\boldsymbol{D}_{\lambda,P}^{\gamma}\boldsymbol{K}\boldsymbol{D}_{\lambda,P}^{\alpha,\beta}, \tag{B4}$$

where $\boldsymbol{x}$ is a $1\times N$ vector of the signal $x(n), -N/2 \leqslant n \leqslant N/2-1$, and $\boldsymbol{K}$ is $N\times M$ matrix. $\boldsymbol{K}_{n,m} = e^{j\pi s\frac{(m-n)^2}{NP}}$, $\boldsymbol{D}_{\lambda,P}^{\gamma}$ and $\boldsymbol{D}_{\lambda,P}^{\alpha,\beta}$ are $N\times N$ and $M\times M$ diagonal matrices, respectively

$$\{\boldsymbol{D}_{\lambda,P}^{\gamma}\}_{n,n} = \{e^{j\pi[\gamma(nT)^2-2\lambda sn-\frac{sn^2}{PN}]}\}_{n=-N/2}^{N/2-1}, \tag{B5}$$

$$\{\boldsymbol{D}_{\lambda,P}^{\alpha,\beta}\}_{m,m} = \{e^{j\pi\alpha(\frac{\lambda}{T|\beta|}-\frac{m}{PNT|\beta|})^2-j\pi s\frac{m^2}{PN}}\}_{m=-M/2}^{M/2-1}. \tag{B6}$$

Then, the Theorem.1 is proved.

Appendix C Implementation of ZDLCT and Sp-LCT

Appendix C.1 Implementation of ZDLCT

The ZDLCT can be implemented by the following steps:

Step 1: Select α, β,γ and the sampling space T, and compute entire frequency interval $[-1/(2T|\beta|), 1/(2T|\beta|)-1/(NT\,|\beta|)]$;

Step 2: Select the frequency subinterval in the LCT domain $[u_1, u_2] \subseteq [-1/(2T|\beta|), 1/(2T|\beta|) - 1/(NT\,|\beta|)]$ and sampling points M, then calculate λ and P based on **Definition 1** and **Definition 2**;

Step 3: Calculate the diagonal matrices $\boldsymbol{D}_{\lambda,P}^{\gamma}, \boldsymbol{D}_{\lambda,P}^{\alpha,\beta}$ and the $N\times M$ matrix $\boldsymbol{K}$;

Step 4: Perform matrix multiplication to obtain the matrix $\boldsymbol{D}_{\lambda,P}^{\gamma}\boldsymbol{K}\boldsymbol{D}_{\lambda,P}^{\alpha,\beta}$;

Step 5: The result of **Step 4** is multiplied by the discrete signal $\boldsymbol{x}$ and the coefficient $\sqrt{\beta}e^{-j\pi/4}$. The output $1\times M$ vector is the ZDLCT of signal $x(n)$ in the selected subinterval $[u_1, u_2]$.

Appendix C.2 Implementation of Sp-LCT

The Sp-LCT can be implemented by the following three steps:

Step 1: Select the specific LCT frequency u_m, and calculated the sequence b_n and the input sequence $x(n)$;

Step 2: Calculate the summation $B(u_m)$ using (7) and (8);

Step 3: Multiply the result of **Step 2** and $Ce^{j\pi\alpha u_m^2}e^{j\pi\beta u_m TN}$ to obtain specific LCT spectrum at frequency u_m in (4).

Appendix D Simulations and comparison of methods

Appendix D.1 ZDLCT Simulations

In this subsection, the ZDLCT will be utilized to refine the spectrum of mono-component and multi-component linear frequency modulation (LFM) signals [7].

Appendix D.1.1 *Spectral refinement of mono-component LFM signal*

Considering a mono-component LFM signal

$$x(t) = e^{j\pi\mu t^2+j2\pi f_0 t}. \tag{D1}$$

The LCT of $x(t)$ is calculated as following

$$L_A[x(t)](u) = \begin{cases} \frac{\sqrt{\beta}}{|\beta|} e^{-\frac{j\pi}{4}} e^{j\pi\alpha u^2} \delta(u - \frac{f_0}{\beta}), & \gamma = -\mu \\ \sqrt{\frac{\beta j}{\gamma+\mu}} e^{-\frac{j\pi}{4}} e^{j\pi\alpha u^2} e^{-\frac{j\pi\beta^2}{\gamma+\mu}(u-\frac{f_0}{\beta})^2}, & \gamma \neq \mu. \end{cases} \tag{D2}$$

It is noted that the mono-component LFM signal has an impulse at $u = \frac{f_0}{\beta}$ under suitable parameters. Thus, we can obtain the initial frequency based on the peak location, that is, $f_0 = u\beta$.

Now we take $f_0 = 0, \mu = 1$ and $A = [3, 2, -1]$, the signal $x(t)$ is band-limited in the interval $[-5, 5]$. The discrete time signal $x(n)$ is sampled from the continuous signal $x(t)$ with sampling interval and the number of sampling point $T = 0.1$ and $N = 100$, respectively. The inherent LCT frequency resolution $T_u = 0.05$ in the whole LCT domain $[-1/(2T|\beta|), 1/(2T|\beta|) - 1/(NT|\beta|)]$. The global spectra of $x(n)$ by DLCT [1] is shown in Fig.D1 (a). Next, we select the local interval $[-0.2970, 0.2970] \subseteq [-1/(2T|\beta|), 1/(2T|\beta|) - 1/(NT|\beta|)]$ to refine the LCT spectrum by the ZDLCT. Fig.D1 (b) presents spectrum on the local range with zoom factor $P = 10$ and shift factor $\lambda = 0$. The results show that we can obtain spectral details, such as the amplitude, width and zero position of the main and side valves, and more accuracy peak value. In addition, for appropriate parameters, we can use the peak to estimate the initial frequency of the LFM signal. Thus, we further consider the effect of spectral refinement on estimated results.

For mentioned above LFM signal and LCT parameters, the estimated value is 0.0495 by using the DLCT, the absolute error is 0.0495. Now we discuss the effects of P, λ and the selected interval on estimated results. When the local interval is $[-0.2970, 0.2970]$, and shift factor is $\lambda = 0$, Fig.D2 shows the peak position of signal $x(t) = e^{j\pi t^2}$ for different P in case of $A = [3, 2, -1]$. These results indicate that for the fixed frequency interval, the larger P value is, the more accuracy the estimation is. However, combining the computational complexity and accuracy, P can not be too large. For appropriate $P = 15$, Fig.D3 shows the estimated value for different local interval and λ. It shows, in the case of sub-intervals containing peaks, that the estimated value is independent of the selected subinterval and λ. In order to demonstrate generality of the algorithm, the estimated initial frequency of LFM signal $x(t)$ in (D1) is shown Table D1 for the suitable P, A and different f_0, μ, where f_i is initial frequency of LFM signals; $\dot{f}$ and $\ddot{f}$ are the estimation of initial frequency of LFM signals based on DLCT and ZDLCT respectively; $\varepsilon_D = |(\dot{f}_i - f_i)/f_i|$ and $\varepsilon_Z = |(\ddot{f}_i - f_i)/f_i|$ represent relative error between the initial frequency and the estimated results. The results indicate that the accuracy of ZDLCT is higher than that of DLCT [1] in some cases. Furthermore, the proposed method can also be applied to refine the spectrum of multi-component LFM signals.

Table D1 The estimate values of initial frequency for different f_0 and μ.

(f_0, μ)	(α, β, γ)	$[u_1, u_2]$	T_u	DLCT [1]		ZDLCT		
				$\dot{f}$	ε_D	P	$\ddot{f}$	ε_Z
$(-10, 1)$	$(2, 2.7, -1)$	$[-0.3839, -0.3544]$	0.0369	-9.9668	0.332%	5	-9.9865	0.1351%
$(-8, 0.3)$	$(2.3, 1.5, -0.3)$	$[-5.413, -5.1949]$	0.033	-7.9922	0.0981%	10	-7.9973	0.0337%
$(-6, -1)$	$(3, 2, 1)$	$[-3.1272, -2.8611]$	0.033	-5.9880	0.2000%	3	-6.0104	0.1733%
$(-4, -1)$	$(3, 8, -2)$	$[-0.5302, -0.4503]$	0.06	-3.9424	1.4400%	10	-3.9624	0.9400%
$(-2, 0.3)$	$(2.3, 1.5, -0.3)$	$[-1.5840, -1.0560]$	0.0660	-1.9800	1.000%	11	-1.9890	0.5500%
$(2, 2)$	$(2, 4, -2)$	$[0.3725, 0.645]$	0.0495	2.0860	4.300%	3	2.0528	2.6400%
$(4, 2)$	$(3, 8 - 2)$	$[0.4503, 0.5302]$	0.0062	4.0424	1.0600%	9	4.0368	0.9200%
$(6, 1)$	$(3, 2, -1)$	$[2.8357, 3.2337]$	0.0498	6.0694	1.1567%	8	6.0198	0.3300%
$(8, 2)$	$(0.1, 4, -2)$	$[1.9154, 2.1144]$	0.0249	8.0596	0.7450%	6	8.0428	0.5350%
$(10, 0.3)$	$(2.3, 1, -0.3)$	$[9.7904, 10.19]$	0.05	9.9902	0.0977%	5	10.0002	0.0022%

Appendix D.1.2 *Spectral refinement of multi-component LFM signal*

Considering the following multi-component LFM signals

$$x(t) = \sum_{i=1}^{m} A_i e^{j2\pi f_i t + j\pi\mu t^2}, \tag{D3}$$

where A_i is the amplitude of *i-th* component, f_i and μ are initial frequency and chirp-rate of *i-th* component, respectively. The LCT of $x(t)$ is given by

$$L_A[x(t)](u) = \begin{cases} \frac{\sqrt{\beta}}{|\beta|} e^{-j\pi(\frac{1}{4} - \alpha u^2)} \sum_{i=1}^{m} A_i \delta(u - \frac{f_i}{\beta}) & \gamma = -\mu \\ \sqrt{\frac{\beta j}{\gamma+\mu}} e^{-j\pi(\frac{1}{4} - \alpha u^2)} \sum_{i=1}^{m} A_i e^{-j\pi\frac{\beta^2}{\gamma+\mu}(u-\frac{f_i}{\beta})^2} & \gamma \neq -\mu. \end{cases}$$

We note that the multi-component LFM signals have m impulses at $u = f_i/\beta$, $i = 1, 2, ..., m$ in the LCT domain for suitable A.

Let $t \in [-5, 5]$, $m = 3$, $[f_1, f_2, f_3] = [2, 2.15, 1]$, $\mu = 1$. We sample $x(t)$ with sampling interval $T = 0.1$ and the number of samples points $N = 100$. The DLCT of $x(n)$ with parameters $\alpha = 2, \beta = 4, \gamma = -1$ can be derived in the whole range

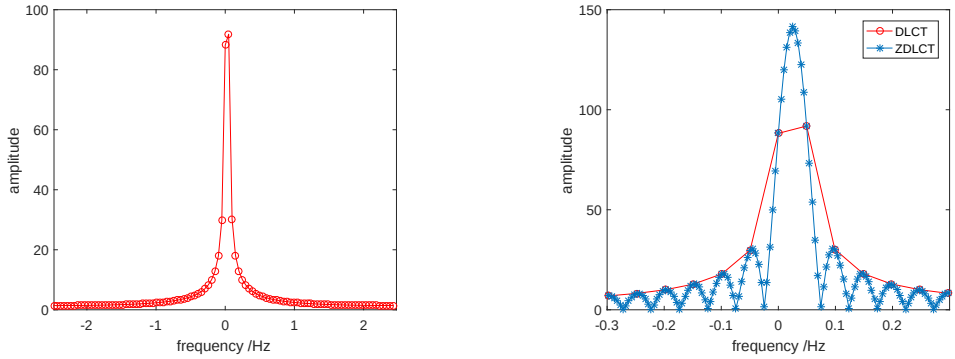

(a) (b)

Figure D1 (a) Global spectrum; (b) The spectrum in the partial range $[-0.2970, 0.2970]$ with $P = 10$.

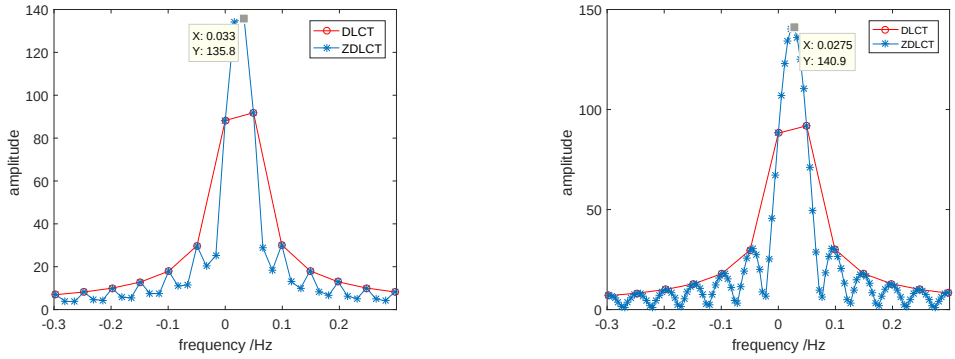

(a) (c)

Figure D2 In local interval $[-0.2970, 0.2970]$, the spectrum with different P: (a) $P = 3$; (c) $P = 9$

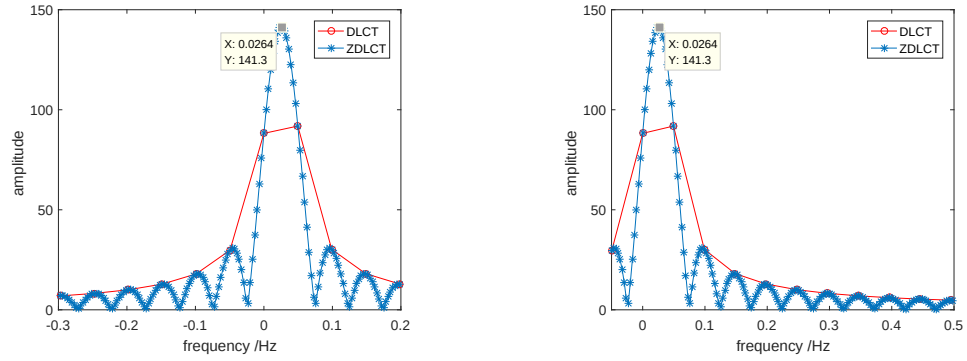

(a) (b)

Figure D3 The spectrum in the different local interval with $P = 15$: (a) $[-0.3960, 0.1980]$ and $\lambda = -0.02$; (b) $[-0.0495, 0.5445]$ and $\lambda = 0.05$.

$[-1.2375, 1.2125]$ with fixed sampling interval $T_u = 0.025$. The global spectrum of $x(n)$ is shown in Fig.D4 (a). The only two peaks can be observed at positions $u_1 = 0.2722, u_2 = 0.5197$, respectively. When the zoom factor $P = 4$ and shift factor $\lambda = 0.11$, the local frequency interval is $[0.1732, 0.6187]$, the LCT spectrum of $x(n)$ by ZDLCT is shown in Fig.D4 (b). It suggests that the closer spectral components can be distinguished by ZDLCT.

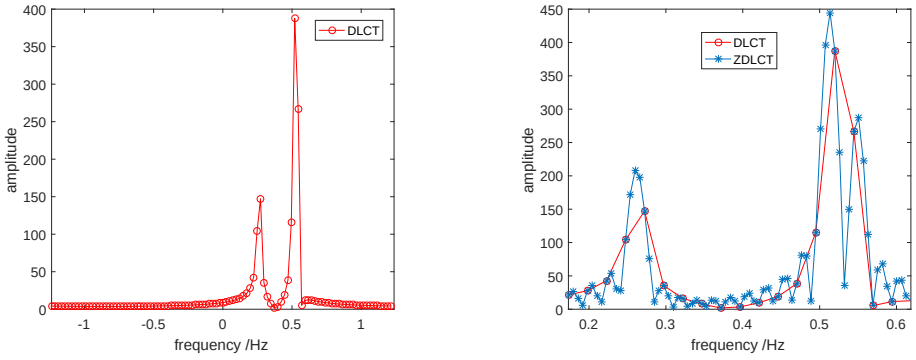

(a) (b)

Figure D4 (a) Global spectrum; (b) The spectrum in the local range $[0.1732, 0.6187]$ with $P = 4$ and $\lambda = 0.11$.

Finally, we consider the effect of spectral refinement on the peak positions of multi-component LFM signal in (D3). Based on obtained the peak position, we can get the estimate values of initial frequency. When the local interval $[0.1732, 0.6187]$ is selected, Table D2 shows estimate values of LFM signal in (D3) for different P. The result demonstrates that the relative error decreases with the increase of P, that is, the same conclusion can be obtained as mono-component LFM signal.

Table D2 The estimate values of initial frequency for different P in the interval$[0.1732, 0.6187]$.

f_i	$P=1$		$P=3$		$P=5$		$P=7$	
	$\dot{f}$	ε_D	$\ddot{f}$	ε_Z	$\ddot{f}$	ε_Z	$\ddot{f}$	ε_Z
$f_1 = 1$	1.0888	8.88%	1.056	5.6%	1.042	4.2%	1.0464	4.64%
$f_2 = 2$	2.0788	3.94%	2.046	2.300%	2.0592	2.96%	2.0508	2.54%
$f_3 = 2.15$			2.2108	2.8279%	2.1976	2.214%	2.192	1.9535%

Appendix D.2 Sp-LCT Simulations

The simulations are performed to verify the accuracy of the Sp-LCT. We consider the following Gaussian signal

$$g(t) = e^{-st^2}. \tag{D4}$$

The continuous LCT of $g(t)$ is given by

$$G_A(u) = L_A[g(t)](u) = \sqrt{\beta} e^{-j\frac{\pi}{4}} \sqrt{\frac{\pi}{s - j\pi\gamma}} e^{\frac{(j\pi\beta u)^2}{s - j\pi\gamma}}. \tag{D5}$$

Appendix D.2.1 *Uniform Sp-LCT*

Let $s = 1/2$ in (D4). Since $e^{-8} \approx 0$, the signal is approximated as finite signal in the interval $[-4, 4]$. The continuous signal $g(t)$ is sampled with sampling interval $T = 0.04$, that is, $g(n) = g(nT)$. We sample the LCT domain variable u with sampling interval $T_u = 0.1244$. The entire amplitude of $g(t)$ by sampled the continuous LCT in (D5), the discrete LCT in (A3) and Sp-LCT with parameters $\alpha = 1/2, \beta = 1, \gamma = 2.5$ are plotted in Fig.D5 (a) in whole LCT domain $[-1/(2T|\beta|), 1/(2T|\beta|) - 1/(NT|\beta|)]$. Fig.D5 (b) shows the local amplitude of $g(n)$ at uniform sampling points $[-1.3681, -0.8706, -0.3731, 0.1244, 0.6219]$ by (A3), (D5) and the Sp-LCT. It shows that the Sp-LCT can effectively obtain a few uniform sampling of output spectrum components. The accuracy is measured by NMSE

$$\text{NMSE} = \frac{\sum \left(|G_A(mT_u)| - |L_A[g(t)](mT_u)|\right)^2}{\sum |G_A(mT_u)|^2}. \tag{D6}$$

The NMSE of Sp-LCT for calculating both all of and local of spectrum are 3.464×10^{-9}. It demonstrated that the DLCT of $g(n)$ computed by the Sp-LCT exactly approximate sampled the continuous LCT of $g(t)$ in (D5).

Appendix D.2.2 *Nonuniform Sp-LCT*

Let $s = \pi$ for $g(t)$ in (D4) with time interval $[-5, 5]$. Here, $g(n) = g(nT)$, $T = 0.05$. We consider the discrete time LCT of $g(n)$ by (A2). The parameters α, β, γ are randomly distributed in the interval $[-5, 5]$, the sampling is nonuniform in

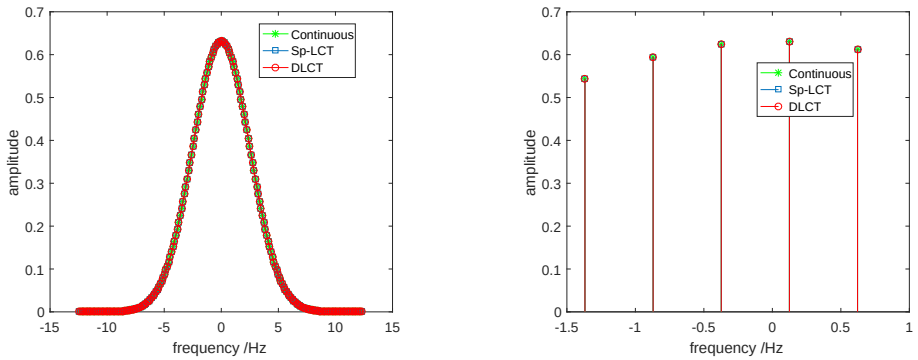

(a) (b)

Figure D5 For $\alpha = 1/2, \beta = 1, \gamma = 2.5$; (a) The amplitude of $g(t)$ by sampled the continuous LCT, DLCT and Sp-LCT in the LCT domain $[-1/(2T\,|\beta|), 1/(2T\,|\beta|) - 1/(NT\,|\beta|)]$; (b) The local amplitude of $g(t)$ by sampled the continuous LCT, DLCT and Sp-LCT at frequency points $[-1.3681, -0.8706, -0.3731, 0.1244, 0.6219]$.

the LCT domain. In order to verify the effectiveness of the Sp-LCT, we adopt $\mathbf{u} = [u_1, u_2, u_3, u_4, u_5, u_6]$, which randomly distributed in the interval $(-2.8429, 2.8144)$. Fig.D6 (a) shows the amplitude of $g(n)$ by Sp-LCT and sampled (D5) at LCT frequency $\mathbf{u}$. We carry out the following NMSE to give a quantitative analysis of the accuracy of Sp-LCT

$$\mathrm{NMSE} = \frac{\sum \left(|G_A(u_m)| - |L_A[g(t)](u_m)|\right)^2}{\sum |G_A(u_m)|^2}. \tag{D7}$$

The simulation runs 500 times independent experiments, the consequences are shown in Fig.D6 (b). The overall trend of the NMSEs for different $\mathbf{u}$ reveals that the NMSEs of the Sp-LCT are below 1.4×10^{-13}. Therefore, the proposed Sp-LCT can approximate the nonuniform sampling of the continuous LCT.

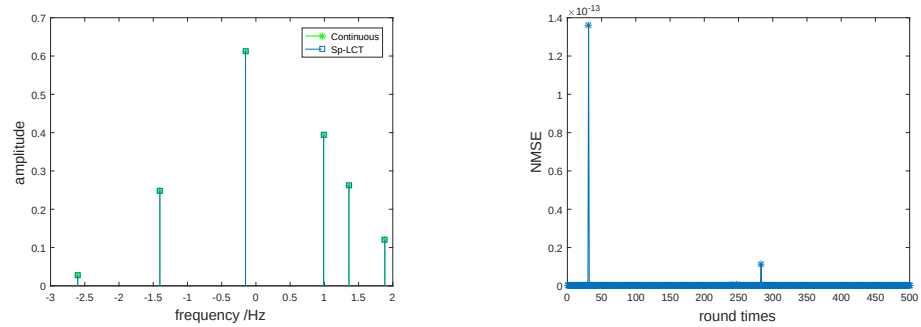

(a) (b)

Figure D6 (a) The amplitude of the continuous LCT and Sp-LCT with parameters α, β, γ which are distributed randomly in the interval $[-5, 5]$ at frequency points $\mathbf{u} = [u_1, u_2, u_3, u_4, u_5, u_6]$; (b) NMSE of the Sp-LCT for 500 different $\mathbf{u}$.

References

1 Hennelly B M, Sheridan J T. Fast numerical algorithm for the linear canonical transform. J Opt Soc Am, 2005, 22: 928-937

2 Zhao J, Tao R, Wang Y. Sampling rate conversion for linear canonical transform. Signal Process, 2008, 88: 2825-2832

3 Pei S C, Ding J J. Closed-form discrete fractional and affine Fourier transforms. IEEE Trans Signal Process, 2000, 48: 1338-1356

4 Zhang F, Tao R, Wang Y. Discrete linear canonical transform computation by adaptive method. Opt Express, 2013, 21: 18138-18151

5 Oktem F S, Ozaktas H M. Exact relation between continuous and discrete linear canonical transforms. IEEE Signal Proc Let, 2009, 16: 727-730

6 Healy J J, Sheridan J T. Sampling and discretization of the linear canonical transform. Signal Process, 2009, 89: 641-648

7 Krini M, Schmidt G. Refinement and temporal interpolation of short-term spectra: theory and applications. New York: Springer, 2014, 139-166